Comparison of Molecular Geometries Determined by Paramagnetic Nuclear Magnetic Resonance Relaxation and Shift Reagents in Solution

D. H. Welti, M. Linder, and R. R. Ernst*

Contribution from the Laboratorium für Physikalische Chemie, Eidgenössische Technische Hochschule, CH-8092 Zürich, Switzerland. Received June 27, 1977

Abstract: The practical use of lanthanide relaxation and shift reagents for the determination of molecular structure in solution is investigated. It is found that in the case of (−)-borneol the geometrical information deduced either from relaxation rate or shift measurements is incompatible, suggesting that different lanthanides can form complexes of different geometry.

Introduction

Lanthanide NMR shift reagents have found widespread use for the determination of molecular geometry in solution.[1-5] Their utility is based on simple relations between the induced paramagnetic shifts and molecular structure. Of particular importance are applications for the structure elucidation of biomolecules.[6,7]

Similar geometrical information can, in principle, also be obtained from lanthanide-induced relaxation rates of the substrate nuclei. Theory again predicts a simple relation between relaxation rate and molecular geometry.

The properties required for ideal shift and relaxation reagents are mutually exclusive, and two different lanthanide chelates have to be employed when both sources of information are required. A shift reagent, Ln^S, must contain a paramagnetic ion with an anisotropic g tensor to cause large paramagnetic pseudocontact shifts and a short electron spin relaxation time to avoid excessive line broadening. A relaxation reagent, Ln^R, on the other hand, should have a long electron spin relaxation time to produce a strong relaxation effect and an isotropic g tensor to permit a simple calculation of the paramagnetic relaxation rate.

La Mar and Faller[8] have suggested treating the substrate with the two lanthanide chelates at the same time. Ln^S will then spread the substrate spectrum such that it becomes first order. Specific relaxation rates can now be attributed to each nucleus, and overlap of the lines broadened by Ln^R will be avoided. Numerous studies have been published combining shift and relaxation information for the elucidation of molecular structure.[9-11]

The observed paramagnetic shifts can in general be caused by the dipolar interaction with a paramagnetic center having an anisotropic g tensor, leading to the pseudocontact shift, and by the scalar contact interaction, leading to the contact shift. For a paramagnetic ion with a g tensor of rotational symmetry, one obtains the shift

$$\left(\frac{\Delta H_i}{H}\right)^S = C_S \left(\frac{1 - 3\cos^2\theta_i}{r_i^3}\right) + \delta_i \tag{1}$$

The first term represents the pseudocontact shift with r_i being the distance of the nucleus i from the paramagnetic ion and θ_i the angle between r_i and the symmetry axis of the g tensor. C_S is a constant which depends on temperature, on concentration, and on the particular ion used. The contact shift δ_i strongly depends on the electronic structure of the complexed molecule and does not follow a simple dependence on geometry. It is often important, particularly for heavier nuclei like carbon-13, phosphorus, and fluorine, as well as for protons in conjugated

systems.[12] However, for the aliphatic system investigated in the present paper it is expected to be unimportant except for protons in the immediate neighborhood of the binding site.[13]

The relaxation rate induced by the added relaxation reagent is usually described by an equation of the form

$$\frac{1}{T_{1_i}^{S+R}} - \frac{1}{T_{1_i}^S} = C_R \left(\frac{1}{r_i^6}\right) + \frac{1}{T_{1\ inter}^R} \tag{2}$$

where superscripts S and R denote relaxation rates in the presence of Ln^S or Ln^R, respectively. $1/T_{1\ inter}^R$ is the intermolecular contribution to relaxation caused by the addition of Ln^R. In analogy to eq 1, contact interaction could, in principle, also contribute to the relaxation rate in eq 2. Again, this contribution is expected to be negligible in the system investigated in this work.

Equation 1 has proved to be satisfactory for the description of the proton shift induced in many substrate molecules. The situation for the relaxation rates is less clear. Apart from Levy's results on the ^{13}C relaxation of borneol,[14] which give only an approximate confirmation, the validity of eq 2 has, to our knowledge, not been tested on a rigid molecule with a suitably high number of nuclei. Some difficulties encountered with the use of relaxation times have recently been pointed out.[15,16]

It is the purpose of this paper to present a critical comparison of structural information obtained from shift and from relaxation rate measurements.[17] A molecule with a rigid frame of known geometry is required to test the compatibility of the information deduced from shift and relaxation time measurements. For the present study, (−)-borneol has been selected. This molecule has been used already by several authors as a model system to study the effects of lanthanide reagents on the chemical shift.[18-25]

Shifts and relaxation rates of the protons in (−)-borneol have been measured for complexes with the ions Eu^{3+}, Pr^{3+}, La^{3+}, and Gd^{3+}. It has been found that the geometrical information deduced from relaxation rate measurements in Gd^{3+} complexes is incompatible with the coordination geometry determined from shift measurements either in Eu^{3+} or Pr^{3+} complexes. It must be concluded that the geometries of different lanthanide complexes can be different.

Paramagnetic Shifts and Relaxation Rates of (−)-Borneol

The assignment of the resonance lines in the proton spectrum of (−)-borneol has been based on the shifts observed in a 360-MHz spectrum and on the spin–spin coupling constants in agreement with the assignment by Briggs et al.[21] The observed shifts of a 0.542 M solution in a mixture of 75 vol %

Table I. Experimental Chemical Shifts for 0.542 M (−)-Borneol in a Mixture of 75 vol % $CDCl_3$ and 25 vol % C_6F_6

Proton	Obsd shift[a]	Obsd shift[a,b]
2-H	4.03	3.90
eq3-H	2.30	2.20
ax3-H	0.94	0.92
4-H	1.63	1.58
eq5-H	1.76	1.70
ax5-H	1.27	1.23
eq6-H	1.25	1.12
ax6-H	1.94	2.03
8-Me	0.90	0.86
9-Me	0.89	0.85
10-Me	0.87	0.82

[a] Chemical shifts in parts per million downfield from internal Me_4Si. [b] Data taken from Briggs et al.[21] (solution in CCl_4).

Table II. Observed Normalized Paramagnetic Shifts of 0.5 M (−)-Borneol with $Eu(fod)_3$-d_{27}

	Normalized shifts[c]				
Proton	60 MHz[a] (45 °C)	60 MHz[a] (45 °C)	360 MHz (32 °C)	Ref 18[b]	Ref 25[b]
2-H	1.000	1.013	0.989	0.974	1.034
eq3-H	0.370	0.379	0.374	0.369	0.338
ax3-H	0.712	0.711	0.721	0.728	0.687
4-H	0.223	0.226	0.229	0.232	0.218
eq5-H	0.247	0.236	0.244	0.245	0.228
ax5-H			0.366	0.369	0.360
eq6-H			0.367	0.369	
ax6-H	0.708	0.692	0.709	0.725	0.674
8-Me	0.168	0.168	0.166	0.166	0.173
9-Me	0.164	0.165	0.164	0.162	0.157
10-Me	0.391	0.386	0.396	0.394	0.357

[a] Values from two different experimental series. [b] No temperature stated. [c] The shift of 2-H in the first series is arbitrarily set equal to 1. The values of the other series have been normalized such that mean square deviations between actual values and those of the first series became minimum.
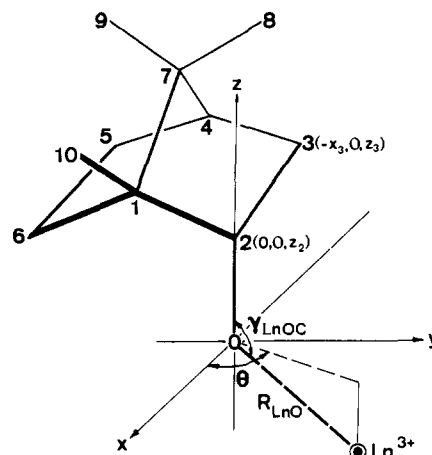
Table III. Observed Diamagnetic Shifts of 0.5 M (−)-Borneol with $La(fod)_3$-d_{27} (360 MHz, 45 °C)

Proton	Obsd shift[a]	Proton	Obsd shift[a]
2-H	+0.29	eq6-H	<0.01
eq3-H	+0.05	ax6-H	−0.52
ax3-H	<0.01	8-Me	<0.01
4-H	+0.02	9-Me	−0.06
eq5-H	+0.05	10-Me	<0.01
ax5-H	+0.19		

[a] Shift in parts per million for hypothetical 1:1 molar ratio of substrate and $La(fod)_3$-d_{27}. Positive values, downfield shifts; negative values, upfield shifts.

Figure 1. Molecular coordinate frame of (−)-borneol and the lanthanide position parameters.

$CDCl_3$ and 25 vol % C_6F_6 are given in Table I together with the values in CCl_4 reported by Briggs et al.[21] The numbering of the carbon centers is indicated in Figure 1.

Table II gives the normalized shifts due to complexation with $Eu(fod)_3$-d_{27}. The values at 60 and 360 MHz agree reasonably well with the values reported by Hawkes et al.[18] and ApSimon et al.[25] Small differences may be due to temperature effects.

The diamagnetic shift due to complexation of (−)-borneol with a lanthanide complex can be judged from the shifts induced by $La(fod)_3$-d_{27}, listed in Table III. These shifts have been used to correct the data of Table II to obtain purely paramagnetic shifts, assuming equal diamagnetic effects for La^{3+} and Eu^{3+}. It has been found that none of these changes is relevant for the determination of the complex geometry ($\Delta R_{LnO} < 0.09$ Å, $\Delta\gamma_{LnOC} < 1.5°$, $\Delta\theta < 0.7°$, compare next section).

The longitudinal relaxation rates for the individual protons in 0.5 M (−)-borneol are listed in Table IV for an europium concentration of 0.25 mol/L and for various mole ratios Gd/Eu. For the evaluation of these relaxation measurements, exponential relaxation of the individual protons has been assumed. No obvious deviation from exponential behavior could be detected. In Table V some relaxation rates for a diamagnetic solution of free (−)-borneol are indicated. It is seen that the various relaxation rates of free (−)-borneol do not differ much.

Although the relaxation rates by europium alone are not expected to strictly obey the $1/r_i^6$ relationship of eq 2 because of the anisotropy of the europium g tensor,[26] intramolecular paramagnetic relaxation should still generate much larger

Table IV. Experimental Longitudinal Relaxation Rates in s^{-1} of 0.5 M (−)-Borneol with 0.25 M $Eu(fod)_3$-d_{27} and Various Mole Ratios Gd/Eu at 45 °C in 75 vol % $CDCl_3$ and 25 vol % C_6F_6

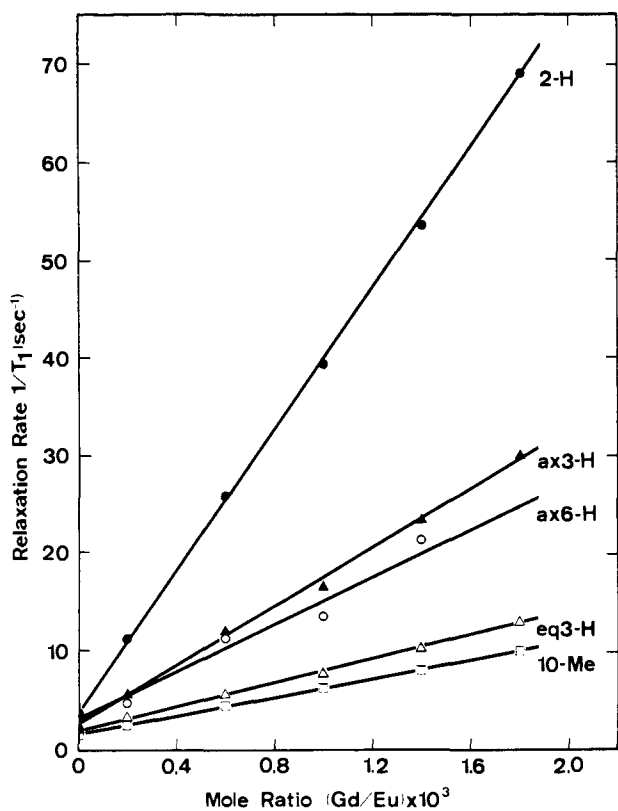|	Mole ratio (Gd/Eu)					
Proton	0.0	0.2×10^{-3}	0.6×10^{-3}	1.0×10^{-3}	1.4×10^{-3}	1.8×10^{-3}
2-H	3.28 ± 0.13	11.34 ± 0.37	26.12 ± 2.44	39.59 ± 3.86	53.86 ± 4.42	69.24 ± 13.35
eq3-H	1.90 ± 0.12	3.43 ± 0.26	5.77 ± 0.14	7.87 ± 0.30	10.39 ± 0.43	13.10 ± 0.41
ax3-H	2.69 ± 0.12	5.74 ± 0.19	12.10 ± 0.64	16.60 ± 0.63	23.59 ± 1.23	30.19 ± 1.32
4-H	1.01 ± 0.06	1.29 ± 0.05	1.92 ± 0.04	2.38 ± 0.05	2.88 ± 0.06	3.53 ± 0.11
eq5-H	1.65 ± 0.21	1.79 ± 0.20	2.59 ± 0.13	3.00 ± 0.15	3.53 ± 0.23	4.09 ± 0.23
ax6-H	3.87 ± 0.72	4.98 ± 0.13	11.09 ± 0.28	13.80 ± 1.51	21.64 ± 3.61	17.13 ± 4.49
8-Me	1.09 ± 0.05	1.36 ± 0.05	2.07 ± 0.06	2.56 ± 0.04	3.16 ± 0.11	3.79 ± 0.15
9-Me	1.17 ± 0.07	1.34 ± 0.05	1.75 ± 0.08	2.04 ± 0.06	2.38 ± 0.06	2.84 ± 0.12
10-Me	1.58 ± 0.03	2.64 ± 0.08	4.64 ± 0.10	6.33 ± 0.08	8.15 ± 0.13	10.03 ± 0.24
fod-H	0.65 ± 0.02	0.71 ± 0.03	0.82 ± 0.02	0.91 ± 0.02	1.01 ± 0.02	1.15 ± 0.06
Me_4Si	0.087 ± 0.012	0.130 ± 0.016	0.197 ± 0.022	0.262 ± 0.018	0.327 ± 0.026	0.412 ± 0.097

Figure 2. Relaxation rates of the protons 2-H, ax3-H, ax6-H, eq3-H, and 10-Me as functions of molar ratio (Gd/Eu). Straight lines shown are least-squares fits to the experimental data.
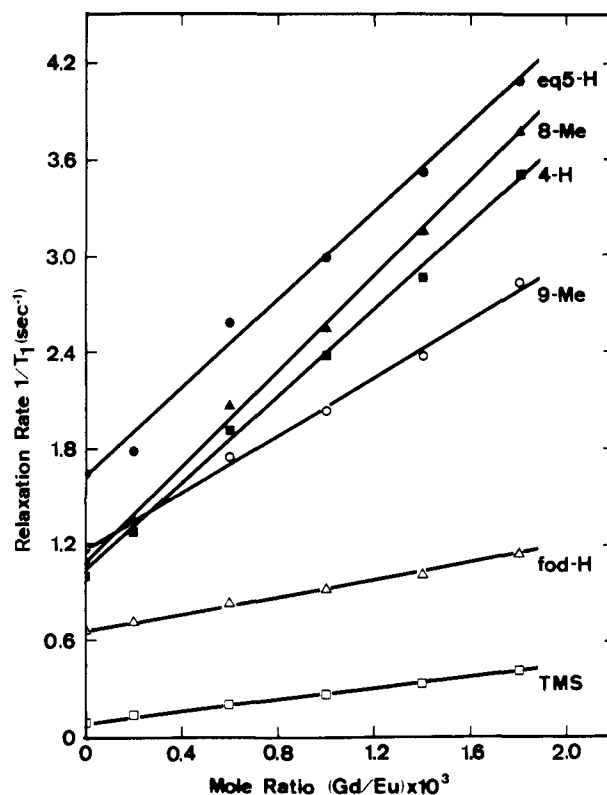

Figure 3. Relaxation rates of the protons eq5-H, 8-Me, 4-H, 9-Me, fod-H, and Me$_4$Si as functions of molar ratio (Gd/Eu). Straight lines shown are least-squares fits to the experimental data.

Table V. Some Longitudinal Relaxation Rates of 0.6 M (−)-Borneol in 75 vol % $CDCl_3$ and 25 vol % C_6F_6

Proton	$1/T_1$, s^{-1}
8,9-Me[a]	0.193 ± 0.016
10-Me	0.213 ± 0.013
−OH[b]	0.185 ± 0.016
Me$_4$Si	0.073 ± 0.016

[a] Signals of 8-Me and 9-Me not separated (60 MHz). [b] Nonexponential relaxation.

Table VI. Longitudinal Relaxation Rates of 0.6 M (−)-Borneol with 0.3 M La(fod)$_3$-d_{27} in 75 vol % $CDCl_3$ and 25 vol % C_6F_6

Proton	$1/T_1$, s^{-1}	Proton	$1/T_1$, s^{-1}
9,10-Me	1.03 ± 0.07	ax6-H	1.59 ± 0.21
8-Me	1.04 ± 0.14	fod-H	0.337 ± 0.066
ax3-H	0.822 ± 0.058	Me$_4$Si	0.086 ± 0.029

relaxation rates for those protons which are near the coordination site than for those far away from it. No effect of the expected magnitude can be observed in the first column of Table IV. The Me$_4$Si relaxation rate of 0.087 ± 0.012 s^{-1} indicates that intermolecular paramagnetic relaxation by Eu^{3+} ions is also relatively unimportant. The relaxation rates of the corresponding lanthanum complex, presented in Table VI, reveal that a major contribution to the increased relaxation rate originates from the dipolar proton–proton relaxation enhanced by the slowdown of molecular motion due to complexing with the bulky lanthanide complex. To eliminate this undesirable effect, which does not contain useful structural information, all Gd-induced relaxation rates used in structural determinations have been corrected by subtracting the relaxation rates of the corresponding Gd^{3+}-free but Eu^{3+}-containing solution,

according to eq 2. As expected, one finds a linear dependence of the relaxation rates induced by Gd^{3+} on its concentration. This is demonstrated by Figures 2 and 3.

Analogous experiments to those with europium and borneol have also been made with praseodymium. The electron spin relaxation time of the latter is somewhat longer, and therefore the paramagnetic relaxation is more important. This can be seen from Table VII, where the normalized shifts and relaxation rates are presented. Again, because of the g tensor anisotropy, the relaxation rates are not expected to follow exactly the simple $1/r_i^6$ dependence and cannot easily be used for the derivation of structural information.

Structure Determination Based on Shifts and on Relaxation Rates

For the structure determination of the Ln(fod)$_3$-(−)-borneol complex, a rigid and known geometry of the borneol frame has been assumed. The proton and oxygen coordinates[27] of borneol, given in Table VIII, were derived from those of camphane derivates determined by Ferguson et al.[28] The three parameters which are required to localize the lanthanide ion, R_{LnO}, γ_{LnOC} and θ, are indicated in Figure 1. For the calculation of the paramagnetic shifts, two assumptions have been made:

(1) *The contact shift is negligible.* There are several indications which justify this assumption. (a) As will be shown later, europium and praseodymium lead, within experimental accuracy, to the same complex geometry. It is known,[29] however, that the contact shift of praseodymium is considerably smaller than that of europium. This suggests that the contact shift does not have a significant influence on the determined geometry. (b) The paramagnetic molar shift of gadolinium, which is exclusively a contact shift, has been found to be at least one order of magnitude smaller than that of europium in similar compounds,[30] leading again to the conclusion that the contact shift is negligible. (c) Elimination of the proton 2-H,

Table VII. Normalized Shifts and Relaxation Rates of 0.6 M (−)-Borneol with 0.3 M Pr(fod)$_3$-d_{27} (60 MHz, 45 °C) in 75 vol % CDCl$_3$ and 25 vol % C$_6$F$_6$

Proton	Normalized shift[a]			Relaxation rates $1/T_1$, s^{-1}
	60 MHz (45 °C)	Ref 18	Ref 25	
2-H	1.000	0.976	1.003	13.38 ± 1.13
eq3-H		0.331	0.356	
ax3-H	0.731	0.740	0.733 ⎫	
4-H	0.225	0.227	⎬ 8.15 ± 0.24	
eq5-H	0.230	0.227	0.209 ⎭ 1.49 ± 0.10	
ax5-H		0.361	0.391	
eq6-H		0.358	0.324	
ax6-H	0.734	0.759	0.732	6.20 ± 0.33
8-Me	0.175	0.166	0.179	1.62 ± 0.10
9-Me	0.165	0.165	0.168	1.45 ± 0.10
10-Me	0.386	0.389	0.387	3.80 ± 0.18
fod-H				13.93 ± 0.16
Me$_4$Si				0.183 ± 0.019

[a] Compare Table II.

Table VIII. Cartesian Coordinates of the Borneol Protons[27] in Å (Figure 1)

Proton	X	Y	Z
2-H	0.449	0.894	1.889
eq3-H	−1.496	0.894	2.597
ax3-H	−2.154	0.000	1.114
4-H	−2.377	−1.254	3.541
eq5-H	−1.476	−3.379	2.659
ax5-H	−2.145	−2.534	1.142
eq6-H	0.471	−3.379	1.951
ax6-H	0.100	−2.536	0.359
8-Me[a]	0.323	0.295	4.572
9-Me[a]	0.335	−2.731	4.606
10-Me[a]	2.486	−1.239	2.023

[a] Average position of methyl protons: intersection point of threefold symmetry axis and plane of the methyl protons.

which is most likely to be susceptible to a contact shift, from the fit of molecular geometry hardly changes the results of the fit.

(2) The *g tensor* of the paramagnetic center has in the time average *rotational symmetry* with respect to the O–Ln bond. It has been pointed out in literature (e.g., ref 31, 32) that the *g* tensor generally lacks rotational symmetry. However, it has been found for (−)-borneol as well as for other molecules (e.g., ref 33) that the experimental shift data can be explained by a *g* tensor of apparent rotational symmetry coaxial with the Ln–O bond. This can be rationalized by assuming an almost unhindered rotation about the Ln–O bond.

The three coordinates of the lanthanide ion in the europium complex have been determined by means of a least-squares fit

for three sets of shift data determined by the present authors as well as for the shift data published by Hawkes et al.[18] and ApSimon et al.[25] The results are given in Table IX. There is a fair agreement among the results from all five data sets. Hawkes et al.[18] have used a different least-squares procedure maximizing the correlation coefficient between calculated and experimental shifts and have in addition varied the direction of the magnetic axis to improve the fit. This explains the slight discrepancies between their and the present fit.

The same procedure has also been used to determine the lanthanide coordinates in the corresponding praseodymium complex. Table IX shows that there is no significant difference between the lanthanide coordinates for the europium and praseodymium complexes.

For the interpretation of the relaxation data in terms of molecular structure, effects not proportional to r_i^{-6} (eq 2) should first be eliminated from the raw data. The following undesirable contributions to relaxation must be considered:

(1) Proton–proton dipolar relaxation. It is governed by the rotational correlation time of the complex, but it is not affected by the very small Gd(fod)$_3$ concentration and is eliminated by subtraction of the relaxation rate $1/T_{1_i}^S$ in the presence of the shift reagent alone, according to eq 2.

(2) Inter- and intramolecular paramagnetic relaxation by Eu(fod)$_3$. It is also eliminated by subtraction of $1/T_{1_i}^S$.

(3) Intermolecular paramagnetic relaxation by Gd(fod)$_3$. Several attempts to eliminate this contribution will be described subsequently.

The following models to describe the intermolecular paramagnetic relaxation by Gd(fod)$_3$ may be considered:

(a) *Me$_4$Si relaxation as a measure for intermolecular paramagnetic relaxation.*[8,14] Because of its similar size, Me$_4$Si may be taken as a probe for intermolecular relaxation for free (−)-borneol. But it must be considered that in the solutions used (−)-borneol is mostly in its complexed form, for which Me$_4$Si is a very poor model.

(b) *Homogeneous relaxation of all protons of (−)-borneol.* An additional free parameter is introduced into the least-squares fit to correct for a constant contribution to all relaxation rates from intermolecular relaxation.

(c) *Sphere model of the Ln(fod)$_3$–borneol complex.* It is assumed that relaxation is dominated by the borneol molecules (S) bound to lanthanide chelates (Ln) in complexes of either LnS or LnS$_2$ stoichiometry:

(1) Lanthanide reagents as well as the complexes LnS and LnS$_2$ are regarded as spheres of radius $R = 8.5$ Å. The gadolinium ions have a homogeneous spatial distribution function outside a sphere of radius $2R = 17$ Å centered at the lanthanide ion, to which the substrate S is coordinated.

(2) The correlation time for intermolecular paramagnetic relaxation is dominated by the Gd^{3+} electron spin relaxation time. This assumption is supported by an estimate of the diffusional correlation time of the complex and of the electron spin relaxation time.[34]

Table IX. Geometric Parameters for Eu^{3+} and Pr^{3+} Calculated Using the Same Fitting Procedure on Different Sets of Shift Data (Tables II and VII)

Shift reagent	R_{LnO}, Å	γ_{LnOC}, deg	θ, deg	Risk function R^a
Eu(fod)$_3$-d_{27}				
60 MHz, 45 °C (set 1)	2.68 ± 0.07	126.9 ± 1.5	90.0 ± 2.1	9.31 × 10^{-5}
60 MHz, 45 °C (set 2)	2.57 ± 0.06	134.2 ± 1.7	95.4 ± 1.5	1.19 × 10^{-4}
360 MHz, 32 °C	2.67 ± 0.04	127.1 ± 0.7	90.8 ± 1.0	1.83 × 10^{-4}
Ref 18	2.58 ± 0.07	128.0 ± 1.4	89.3 ± 1.8	2.05 × 10^{-4}
Ref 25	2.70 ± 0.09	127.5 ± 1.8	92.3 ± 2.4	1.75 × 10^{-4}
Pr(fod)$_3$-d_{27}				
60 MHz, 45 °C	2.61 ± 0.08	128.8 ± 1.6	93.3 ± 2.5	1.77 × 10^{-4}
Ref 18	2.50 ± 0.07	128.2 ± 1.4	93.3 ± 1.9	2.71 × 10^{-4}

[a] See Experimental Section for the definition of the risk function R.
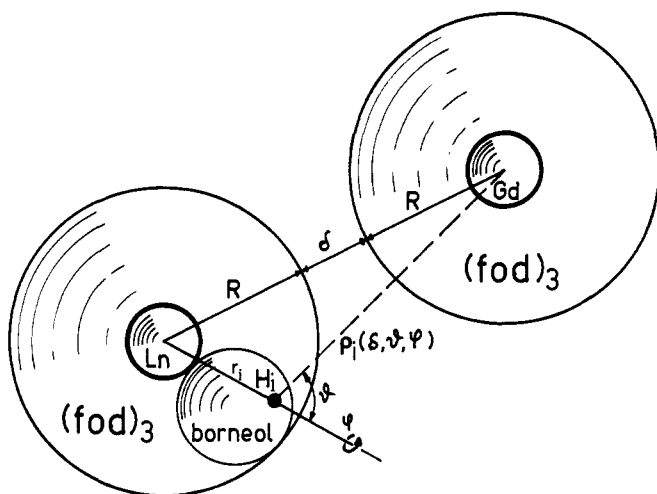
Figure 4. Hard sphere model of [Ln(fod)$_3$-d_{27}-borneol]-[Gd(fod)$_3$-d_{27}] interaction.

(3) The intermolecular paramagnetic relaxation of free borneol is neglected, as it gives at most a small, approximately constant contribution to all relaxation rates.

This model is schematically shown in Figure 4. It is seen that the minimal distance of approach for the gadolinium ion is considerably smaller for the substrate protons lying near the surface of the sphere, away from the binding site. Therefore, the contribution of the intermolecular paramagnetic relaxation is dependent on the position of the proton in complexed borneol. The intermolecular relaxation rates have been computed for each proton by integration over the spatial distribution function of the gadolinium ions in solution:

$$1/T_{1\ \text{inter}_i}^{R} = C_R' \int_{(\delta>0)} \frac{1}{\rho_i^6(\delta,\vartheta,\varphi)} \, dV \quad (3)$$

For a specific proton i of a borneol molecule, coordinated to a lanthanide ion at a distance r_i, the lower limit of the distance ρ_i from the proton to a gadolinium ion in solution is $2R - r_i$. Within the range of $2R - r_i < \rho_i < 2R + r_i$, the angle ϑ is limited to $0 \leq \vartheta \leq \text{arc cos} \ [(4R^2 - r_i^2 - \rho_i^2)/2r_i\rho_i]$.

This leads to the following sum of two integrals:

$$\frac{1}{T_{1\ \text{inter}_i}^{R}} = \int_{2R-r_i}^{2R+r_i} \rho_i^2 \, d\rho_i$$

$$\times \int_0^{\text{arc cos}(4R^2-r_i^2-\rho_i^2/2r_i\rho_i)} \sin \vartheta \, d\vartheta \int_0^{2\pi} d\varphi \left(\frac{C_R'}{\rho_i^6}\right)$$

$$+ \int_{2R+r_i}^{\infty} \rho_i^2 \, d\rho_i \int_0^{\pi} \sin \vartheta \, d\vartheta \int_0^{2\pi} d\varphi \left(\frac{C_R'}{\rho_i^6}\right) \quad (4)$$

The analytical result of the integration is

$$\frac{1}{T_{1\ \text{inter}_i}^{R}} = C_R'\pi \left\{ \frac{4R^2 - r_i^2}{4r_i} [(2R + r_i)^{-4} \right.$$

$$- (2R - r_i)^{-4}] + \frac{2}{3} [(2R + r_i)^{-3} + (2R - r_i)^{-3}]$$

$$\left. - \frac{1}{2r_i} [(2R + r_i)^{-2} - (2R - r_i)^{-2}] \right\} \quad (5)$$

The constant C_R' must be taken into the least-squares fit procedure as a fourth parameter besides R_{LnO}, γ_{LnOC}, and θ.

All three models have been tried to fit the experimental relaxation rates. Model (a) did not give a satisfactory correlation with the expected $1/r_i^6$ dependence, producing differences between calculated and measured relaxation rates of up to 45% and an unreasonably large bond length R_{LnO} of 3.3 Å. This poor fit is understandable. Free Me$_4$Si is an inadequate model for the complexed (−)-borneol because it is approached more easily by other lanthanide reagent molecules and because of its shorter translational correlation time.

Both models (b) and (c) produce a satisfactory fit of experimental and theoretical relaxation rates. The results of the least-squares fit are given in Tables X and XI for three mole ratios Gd/Eu using experimental data from Table IV. There is neither a significant difference between the values obtained with the two models nor a clear tendency of the geometric parameters as a function of concentration.

It is found that the relaxation rates are quite sensitive to changes in the angles γ_{LnOC} and θ but do not vary much with R_{LnO}. This is reflected in the small error limits of the angles and in the large uncertainty of R_{LnO} (Tables X and XI). The unreasonably small value of R_{LnO} may, to some extent, be

Table X. Geometric Parameters for Gd^{3+} and Values for $1/T_{1\ \text{inter}}$ (Model (b)) Calculated from Relaxation Data (Table IV)

	Mole ratio (Gd/Eu)		
	0.6×10^{-3}	1.0×10^{-3}	1.4×10^{-3}
R_{LnO}, Å	1.56 ± 0.22	1.82 ± 0.23	1.75 ± 0.22
γ_{LnOC}, deg	141.2 ± 2.2	137.2 ± 2.7	138.1 ± 2.8
θ, deg	66.8 ± 2.6	67.5 ± 2.1	69.2 ± 2.2
$1/T_{1\ \text{inter}}$, s^{-1}	0.450 ± 0.165	0.607 ± 0.221	0.817 ± 0.262
Risk function R^a	2.17×10^{-3}	1.91×10^{-3}	4.26×10^{-3}
Corr coeff^b (R_{LnO}, $1/T_{1\ \text{inter}}$)	-0.970	-0.976	-0.958

^{a} See Experimental Section for the definition of the risk function R. ^{b} Correlation coefficient between the two parameters R_{LnO} and $1/T_{1\ \text{inter}}$.

Table XI. Geometric Parameters for Gd^{3+} and Values for $1/T_{1\ \text{inter}_i}$ (Model (c)) Calculated from Relaxation Data (Table IV)

	Mole ratio (Gd/Eu)		
	0.6×10^{-3}	1.0×10^{-3}	1.4×10^{-3}
R_{LnO}, Å	1.66 ± 0.23	2.06 ± 0.26	1.96 ± 0.23
γ_{LnOC}, deg	141.5 ± 2.2	137.5 ± 2.7	138.2 ± 2.7
θ, deg	67.3 ± 2.5	60.0 ± 2.0	70.6 ± 1.9
$1/T_{1\ \text{inter}_i}$, s^{-1} ^{a}	$0.310/0.482$	$0.366/0.600$	$0.498/0.806$
	$(\pm42.0\%)$	$(\pm45.4\%)$	$(\pm37.9\%)$
Risk function R	3.25×10^{-3}	4.21×10^{-3}	8.45×10^{-3}
Corr coeff (R_{LnO}, $1/T_{1\ \text{inter}_i}$)	-0.976	-0.982	-0.966

^{a} Lower limit corresponding to $1/T_{1\ \text{inter}_{2-H}}$. Upper limit corresponding to $1/T_{1\ \text{inter}_{9-Me}}$.

Table XII. Geometric Parameters for Eu^{3+} and Pr^{3+} Calculated from Shift Data (Two Discrete θ Values Assumed)

Shift reagent	R_{LnO}, Å	γ_{LnOC}, deg	θ_1, deg (population)	θ_2, deg (population)	Risk function R
$Eu(fod)_3$-d_{27}					
60 MHz, 45 °C (set 1)	2.62 ± 0.09	125.9 ± 1.4	84.3 ± 2.5 (94.4%)	184.4 ± 20.6 (5.6%)	5.81×10^{-5}
60 MHz, 45 °C (set 2)	2.62 ± 0.13	126.0 ± 1.5	82.1 ± 2.4 (93.4%)	199.7 ± 15.3 (6.6%)	4.44×10^{-5}
360 MHz, 32 °C	2.61 ± 0.04	125.7 ± 0.7	84.5 ± 1.2 (95.2%)	181.3 ± 7.0 (4.8%)	1.26×10^{-4}
Ref 18	2.53 ± 0.07	126.4 ± 1.3	84.2 ± 2.1 (96.4%)	190.6 ± 13.6 (3.6%)	1.53×10^{-4}
$Pr(fod)_3$-d_{27}					
60 MHz, 45 °C	2.54 ± 0.11	127.1 ± 1.3	80.0 ± 3.1 (91.3%)	201.8 ± 7.7 (8.7%)	7.68×10^{-5}
Ref 18	2.42 ± 0.07	126.5 ± 1.2	87.5 ± 1.9 (96.9%)	207.1 ± 9.6 (3.1%)	1.99×10^{-4}

Table XIII. Geometric Parameters for Gd^{3+} and Values for $1/T_{1\ inter_i}$ (Model (c)) Calculated from Relaxation Data (Two Discrete θ Values Assumed)

	Mole ratio (Gd/Eu)		
	0.6×10^{-3}	1.0×10^{-3}	1.4×10^{-3}
R_{LnO}, Å	2.62 ± 0.54	2.39 ± 0.34	2.52 ± 0.25
γ_{LnOC}, deg	123.6 ± 9.1	129.5 ± 6.7	124.1 ± 5.7
θ_1, deg (population)	65.9 ± 2.3 (94.9%)	66.6 ± 2.8 (96.5%)	66.3 ± 2.3 (94.7%)
θ_2, deg (population)	216.4 ± 2.2 (5.1%)	216.9 ± 5.8 (3.5%)	219.4 ± 4.0 (5.3%)
$1/T_{1\ inter_i}$, s^{-1} [a]	$0.219/0.377$ ($\pm72.8\%$)	$0.325/0.548$ ($\pm47.1\%$)	$0.417/0.708$ ($\pm33.0\%$)
Risk function R	9.11×10^{-4}	2.76×10^{-3}	4.22×10^{-4}
Corr coeff (R_{LnO}, $1/T_{1\ inter_i}$)	-0.953	-0.903	-0.816

[a] Lower limit corresponding to $1/T_{1\ inter_{2-H}}$. Upper limit corresponding to $1/T_{1\ inter_{9-Me}}$.

caused by the fitting procedure. It can be seen that there is a very high correlation between R_{LnO} and the intermolecular relaxation rates used in the fit.

The coordinates gained from the relaxation rates call for a comparison with the values obtained from the shift measurement, given in Table IX. One finds that there are significant differences between the complex geometries determined from shift and from relaxation measurements. The angle θ is most significantly changed, being about 23° smaller for the relaxation data than for the shift data. The angle γ_{LnOC}, on the other hand, is approximately 10° larger when determined from the relaxation data. Finally, there is also a drastic difference in the bond length R_{LnO}. The relaxation data imply a bond length shorter by about 0.8 Å.

Several attempts have been made to reconcile the results obtained from shift and relaxation measurements:

(1) R_{LnO} has been given a fixed value of 2.5 Å, and the angles γ_{LnOC} and θ were optimized fitting the relaxation data whereby the two angles change only insignificantly. This implies that the uncertainty in R_{LnO} does not influence the accuracy of the angles.

(2) A dynamic description of the lanthanide complex has been used with some internal motional degree of freedom of the complex. It is to be expected that primarily the angle θ is involved in an internal large amplitude motion. A Gaussian distribution of the angle θ with variable width has been introduced to compute the average expressions

$$\left\langle \frac{1 - 3\cos^2\theta_i}{r_i^3} \right\rangle \text{ and } \left\langle \frac{1}{r_i^6} \right\rangle$$

for the computation of shift and relaxation rates, respectively. On no account, a satisfactory fit could be found when relaxation and shift data have been used simultaneously, whereas separate fitting led to coordinates very similar to those of Tables IX-XI.

(3) Stilbs[35] has recently proposed to use a model with two discrete conformations of the complex with different values of the angle θ and fast exchange between the two conformations. Based on the chemical shift data of ref 21 and 22, he found two conformations with much different populations. This model has been used to fit shift and relaxation data of the present investigation separately. The results are contained in Tables XII and XIII. Naturally, the fit improves as two new free parameters are introduced.

The difference between the bond lengths R_{LnO} determined from shift or from relaxation rate data becomes now insignificant. The angle γ_{LnOC} is also equal within the error limits for both fits. But the most significant difference, the incompatibility of the angle θ_1 of the predominant conformation (93–99%), remains. The angle θ_2 of the low-abundance conformation (1–7%) assumes a completely unreasonable value of $\theta_2 \approx 200°$. A comparison with a molecular model immediately shows that the lanthanide–proton distances become much too short for a realistic molecular conformation.

(4) It could be expected that shift and relaxation rate of proton 2-H are affected by some contact interaction despite the arguments given at the beginning of this chapter. Fitting the data with exclusion of proton 2-H, however, does not lead to significantly different results.

Thus, none of the attempted refinements lead to a satisfactory simultaneous fit of shift and relaxation data.

Discussion

An interpretation of the discrepancy between the results based on shift or relaxation rate data will now be attempted. It is quite obvious that a sufficiently sophisticated model with a sufficient number of parameters would permit a simultaneous satisfactory fit of both sets of data. It is most logical to consider for this purpose a dynamic model with a continuous or discrete distribution of complex conformations. Two simple examples

of this type have been mentioned in the preceding section. Both did not yet permit a perfect fit and more free parameters would have to be introduced. According to the experience gained during the described work, it is rather unlikely that such an artificial refinement would lead to a physically reasonable model of the complex.

It is known that Ln(fod)$_3$ forms both 1:1 and 1:2 complexes with various organic substrates (compare, e.g., ref 36). It cannot therefore be excluded that particularly at low concentration of lanthanides significant concentrations of LnS$_2$ complexes are present. This can also be inferred from the measured concentration dependence of the paramagnetic shift of (−)-borneol.[44] In addition it cannot be excluded that the coordination geometry of (−)-borneol in the LnS and LnS$_2$ complexes is different due to steric hindrance and due to electronic effects. A two-site model would then be necessary to obtain a satisfactory fit of shifts and relaxation rates. As mentioned before, such a fit using two different values of the most sensitive coordinate θ did not lead to a significant improvement. This suggests similar coordination geometries of 1:1 and 1:2 complexes. Therefore a comparison of shift and relaxation data at the same concentration should not be strongly affected by the LnS–LnS$_2$ equilibrium.

Another possibility which cannot completely be excluded is the formation of oligomers by self-association of lanthanide complexes.[37-40] This would give rise to additional "external" relaxation.

However, we believe that the observed discrepancy must be interpreted rather in terms of a different binding geometry of the gadolinium and europium complexes. The gadolinium complex shows then a significantly smaller angle θ by about 23°. This is not completely surprising as this angle is not so much determined by electronic effects of chemical bonds but much more by the hindrance of rotation by the bulky ligands of the lanthanide complex. A small change of the chelate geometry may have a large effect on the angle θ.

These findings are in contrast to previous[18,25] and the present measurements, comparing the geometries of europium and praseodymium complexes which have been found to be identical within the experimental error limits.

It would therefore be interesting to use relaxation rate and shift measurements on the same lanthanide complex to determine the compatibility of the two measurements. This is, unfortunately, difficult, because the required properties of the paramagnetic ion are mutually exclusive, as has been mentioned in the Introduction. There is also little hope that the complex geometry in solution could be determined with sufficient accuracy by another technique presently available.

Whatever the interpretation of the found discrepancies is, it implies that relaxation data cannot always be used to derive geometrical molecular information compatible with that derived from shift measurements.

In addition, it has to be remembered that the relaxation rates are sensitive to several additional factors which must be considered whenever quantitative molecular information is desired. This is to some extent caused by the very strong $1/r^6$ dependence of the paramagnetic relaxation rate which makes protons remote from the paramagnetic center relatively sensitive to other relaxation mechanisms. Of importance are here the *intra*molecular dipolar proton–proton relaxation enhanced by the lengthening of the rotational correlation time upon binding to the complex, and the *inter*molecular paramagnetic relaxation due to the paramagnetic centers in other molecules. The latter will not affect all substrate protons to the same extent because of the different accessibility of various protons. In addition, protons near the paramagnetic center may also experience some relaxation by contact interaction and in certain cases cross relaxation between adjacent protons may play an important role, although a theoretical analysis[34] has shown

that cross relaxation is negligible for (−)-borneol under the present circumstances.

It must, therefore, be concluded that relaxation rates have to be used with particular care whenever quantitative information is to be deduced. Nevertheless, they are in many cases a convenient qualitative measure for the conformations of substrate molecules. To test whether these findings apply to a larger class of systems, it would be of great interest to extend these studies to other lanthanide ions, and also to other ligands with and without internal degrees of freedom.

Experimental Section

Sample Preparation. Commercially available chemicals were used with additional purification. La(fod)$_3$-d_{27} was prepared from La(NO$_3$)$_3$ and Hfod-d_9 according to the procedure of Springer, Meek, and Sievers.[41] After sublimation, the lanthanide reagents were stored over P$_2$O$_5$ in a vacuum desiccator prior to use.

The solvent, a mixture of 75 vol % CDCl$_3$ (with Me$_4$Si) and 25 vol % C$_6$F$_6$, was dried over Linde molecular sieves. Hexafluorobenzene was used as frequency standard for the ^{19}F heteronuclear field frequency lock system.

The samples were prepared in a drybox under nitrogen, degassed, and sealed.

Spin–Lattice Relaxation Measurements. Proton spin–lattice relaxation times were obtained at 45 °C from nonselective inversion-recovery experiments[42] performed on a modified Varian DA-60 spectrometer (60 MHz, ^{19}F heterolock system), which was controlled by a Varian 620/L-100 computer with 16K core memory and a Diablo disk unit as external storage.

In order to minimize slow spectrometer drifts and to improve the signal to noise ratio, a special time averaging procedure was used in which whole series of 180°-τ-90° experiments with up to 20 different pulse delays τ were repeated as many times as necessary, using the disk unit as an intermediate storage. For the removal of the effects of residual transverse magnetization after an imperfect 180° pulse either a homospoil pulse or a pseudostochastic delay of the 90° pulse was employed.[43] The FIDs (4096 samples) were apodized with a cosine weight function, Fourier transformed, and phase adjusted.

The intensities of the spectral lines were determined either from the height of the signal or, for well-separated and not too broad lines, by numerical integration. The relaxation rates and their standard deviations were then calculated with a weighted least-squares Fortran program.

Determination of Lanthanide-Induced Shifts. Shift measurements were made on a Bruker HX 360 spectrometer and on a modified Varian DA-60 spectrometer.

The normalized paramagnetic shifts used for the quantitative calculations in this study were obtained by a linear least-squares analysis of the chemical shifts as functions of the lanthanide concentration at molar ratios ≤0.45.

Optimization of the Lanthanide Position. A weighted least-squares procedure was utilized to minimize the risk function

$$R = \sum_{i=1}^{N} \left(\frac{x_i^{\text{obsd}} - x_i^{\text{calcd}}}{\sigma_i} \right)^2 \sum_{i=1}^{N} \sigma_i^2$$

as a function of the lanthanide coordinates R_{LnO}, γ_{LnOC}, and θ, with x_i^{obsd} being either measured molar paramagnetic shifts or corrected paramagnetic relaxation rates. Other risk functions with modified weighting have been used without obtaining significantly different results. The variance σ_i was estimated from repeated experiments. In some cases, additional molecular parameters were introduced and optimized as well in the least-squares procedure.

References and Notes

(1) R. E. Sievers, Ed., "Nuclear Magnetic Resonance Shift Reagents", Academic Press, New York, N.Y., 1973.
(2) R. v. Ammon and R. D. Fischer, *Angew. Chem.*, **84**, 737 (1972).
(3) G. N. La Mar, W. DeW. Horrocks, Jr., and R. H. Holm, Ed., "NMR of Paramagnetic Molecules: Principles and Applications", Academic Press, New York, N.Y., 1973.
(4) A. F. Cockerill, G. L. O. Davies, R. C. Harden, and J. M. Rackham, *Chem. Rev.*, **73**, 553–588 (1973).
(5) J. Reuben, *Prog. Nucl. Magn. Reson. Spectrosc.*, **9**, 1–70 (1973).
(6) R. A. Dwek, "Nuclear Magnetic Resonance in Biochemistry", Clarendon Press, Oxford, 1973.
(7) R. A. Dwek, *Adv. Mol. Relaxation Processes*, **4**, 1–53 (1972).
(8) G. N. La Mar and J. W. Faller, *J. Am. Chem. Soc.*, **95**, 3817 (1973).
(9) J. Reuben and J. S. Leigh, *J. Am. Chem. Soc.*, **94**, 2789 (1972).
(10) C. M. Dobson, R. J. P. Williams, and A. V. Xavier, *J. Chem. Soc., Dalton Trans.*, 1762 (1974); C. D. Barry, C. M. Dobson, R. J. P. Williams, and A. V. Xavier, *ibid.*, 1765 (1974); C. M. Dobson, L. O. Ford, S. E. Summers, and R. J. P. Williams, *J. Chem. Soc., Faraday Trans. 2*, 1145 (1975).
(11) R. E. Lenkinski and J. Reuben, *J. Am. Chem. Soc.*, **98**, 4065 (1976).
(12) C. N. Reilley, B. W. Good, and R. D. Allendoerfer, *Anal. Chem.*, **48**, 1446 (1976).
(13) W. DeW. Horrocks, Jr., ref 3, p 479.
(14) G. C. Levy and R. A. Komoroski, *J. Am. Chem. Soc.*, **96**, 678 (1974).
(15) J. W. Faller, M. A. Adams, and G. N. La Mar, *Tetrahedron Lett.*, **9**, 699 (1974).
(16) G. N. La Mar and E. A. Metz, *J. Am. Chem. Soc.*, **96**, 5611 (1974).
(17) Preliminary results have been presented by one of the authors (D.W.) at the Third International Meeting on NMR Spectroscopy, St. Andrews, Scotland, July 1975.
(18) G. E. Hawkes, D. Leibfritz, D. W. Roberts, and J. D. Roberts, *J. Am. Chem. Soc.*, **95**, 1659 (1973).
(19) P. V. Demarco, T. C. Elzey, R. B. Lewis, and E. Wenkert, *J. Am. Chem. Soc.*, **92**, 5734 (1970).
(20) J. Goodisman and R. S. Matthews, *J. Chem. Soc., Chem. Commun.*, 127 (1972).
(21) J. M. Briggs, F. A. Hart, and G. P. Moss, *Chem. Commun.*, 1506 (1970).
(22) J. M. Briggs, F. A. Hart, G. P. Moss, and E. W. Randall, *Chem. Commun.*, 364 (1971).
(23) J. M. Briggs, F. A. Hart, G. P. Moss, E. W. Randall, K. D. Sales, and M. L. Staniforth, ref 1, p 197.
(24) W. DeW. Horrocks, Jr., ref 3, p 506.
(25) J. W. ApSimon and H. Beierbeck, *Tetrahedron Lett.*, **8**, 581 (1973).
(26) H. Sternlicht, *J. Chem. Phys.*, **42**, 2250 (1965).
(27) J. D. Roberts, private communication.
(28) G. Ferguson, C. J. Fritchie, J. M. Robertson, and G. A. Sim, *J. Chem. Soc.*, 1976 (1961).
(29) J. Reuben and D. Fiat, *J. Chem. Phys.*, **51**, 4909 (1969).
(30) J. Karhan and R. R. Ernst, unpublished measurements.
(31) R. M. Wing, J. J. Uebel, and K. K. Andersen, *J. Am. Chem. Soc.*, **95**, 6046 (1973).
(32) T. D. Marinetti, G. H. Snyder, and B. D. Sykes, *J. Am. Chem. Soc.*, **97**, 6562 (1975).
(33) H. L. Ammon, P. H. Mazzocchi, W. J. Kopecky, Jr., H. J. Tamburin, and P. H. Watts, Jr., *J. Am. Chem. Soc.*, **95**, 1968 (1973).
(34) D. Weltl, Dissertation No. 5704, ETH Zürich, 1976.
(35) P. Stilbs, *Chem. Scr.*, **7**, 59 (1975).
(36) M. D. Johnston, B. L. Shapiro, M. J. Shapiro, T. W. Proulx, A. D. Godwin, and H. L. Pearce, *J. Am. Chem. Soc.*, **97**, 542 (1975).
(37) C. C. Hinckley, W. A. Boyd G. V. Smith, and F. Behbahany, ref 1, p 1.
(38) D. S. Dyer, J. A. Cunningham, J. J. Brooks, R. E. Sievers, and R. E. Rondeau, ref 1, p 21.
(39) R. B. Lewis and E. Wenkert, ref 1, p 99.
(40) C. S. Springer, A. H. Bruder, S. R. Tanny, M. Pickering, and H. A. Rockefeller, ref 1, p 283.
(41) C. S. Springer, Jr., D. W. Meek, and R. E. Sievers, *Inorg. Chem.*, **6**, 1105 (1967).
(42) R. L. Vold, J. S. Waugh, M. P. Klein, and D. E. Phelps, *J. Chem. Phys.*, **48**, 3831 (1968).
(43) R. Freeman and H. D. W. Hill, *J. Magn. Reson.*, **4**, 366 (1971).
(44) M. Linder, Diploma Thesis, ETH Zürich, 1976.

Interpretation of Complex Molecular Motions in Solution. A Variable Frequency Carbon-13 Relaxation Study of Chain Segmental Motions in Poly(*n*-alkyl methacrylates)

George C. Levy,[*1] David E. Axelson,[*] Robert Schwartz, and Jiri Hochmann

Contribution from the Department of Chemistry, Florida State University, Tallahassee, Florida 32306. Received May 11, 1977

Abstract: An extensive variable temperature study of poly(*n*-butyl methacrylate) and poly(*n*-hexyl methacrylate) at two widely separated frequencies (67.9 and 22.6 MHz) has revealed that a model requiring a nonexponential autocorrelation function, or, its mathematical equivalent, a distribution of correlation times, describes the NMR parameters obtained for the backbone carbons. However, frequency-dependent spin–lattice relaxation time (T_1) and nuclear Overhauser effect (NOE) behavior observed for all side-chain carbons, including the terminal methyls, with NT_1s of the order of 20 s, could not be described in terms of present theoretical approaches. A new model developed retains the distribution of correlation times for the backbone carbons and incorporates the effects of multiple internal rotations about the carbon–carbon single bonds for the side-chain carbons. This model predicts a substantial frequency dependence for broad distribution widths which can quantitatively reproduce almost all of the observed data. For the highest temperatures attained ($\sim$110 °C) the observed T_1 frequency dependence is quite large and only semiquantitatively accounted for using this modified theory. The ramifications of multifrequency experiments with respect to the proper interpretation of complex motions are explored.

Introduction

As equipment and relaxation measurement techniques have become more sophisticated and sensitive in the last few years, the amount of molecular dynamics information which can be obtained by NMR has increased greatly.[2–5] However, as these experiments become more accurate, the possibility of elucidation of more subtle molecular dynamic processes is enhanced. These additional consequences of the development of the field result in other problems, namely, the analysis of any relaxation data presupposes that an adequate model has been chosen. The generally accepted approximation of a single correlation time characterizing the exponential decay of the autocorrelation function has been the choice of preference for most analyses.[6–13]

Theoretical advances[14–23] have allowed for the interpretation of more complex molecular motions but extensive variable temperature and variable frequency experiments have not been available to properly test the various models. Such testing should encompass measurement of all three accessible parameters, the spin–lattice relaxation time, T_1, the spin–spin relaxation time, T_2, and the nuclear Overhauser enhancement, NOE. However, the more stringent experimental requirements